

The magnetic phase diagram of cobalt-manganese alloys

A. Z. Men'shikov, G. A. Takzei, Yu. A. Dorofeev, V. A. Kazantsev, A. K. Kostyshin, and I. I. Sych

Institute of Metal Physics, Ural Scientific Center of the Academy of Sciences of the USSR, Sverdlovsk

(Submitted 18 March 1985)

Zh. Eksp. Teor. Fiz. **89**, 1269–1279 (October 1985)

The magnetic phase diagram of $\text{Co}_{1-x}\text{Mn}_x$ alloys has been studied by magnetic and neutron diffraction methods. The boundaries of the γ - ϵ structural transformation were determined and the regions of existence of ferromagnetic ($0 \leq x \leq 0.25$) and antiferromagnetic ($0.42 < x \leq 0.52$) long-range order were found. A new state (superantiferromagnetism) was found which is an antiferromagnet broken up into finely divided regions with dimensions ~ 8 – 10 nm, in a paramagnet matrix above the Néel temperature or of the temperature of superantiferromagnetic cluster blocking. A region of tricritical behavior with respect to ferromagnetism and antiferromagnetism was noted. It is shown that on lowering the temperature the superparamagnetic and superantiferromagnetic states are frozen-in by gradual blocking of the ferro- and antiferromagnetic clusters respectively. The $\text{Co}_{1-x}\text{Mn}_x$ system of alloys can be regarded as typical Ising magnetic materials in which exchange interaction of the $J_{\text{CoCo}} > 0$, $J_{\text{CoMn}} < 0$, $J_{\text{MnMn}} < 0$ type takes place.

Magnetic phase diagrams of random systems with competing exchange interactions between the atoms are of interest in connection with problems of the magnetic states which arise in near the transition from ferromagnetism to antiferromagnetism. Such transitions could be realized within the bounds of the fcc crystal lattice in the ternary alloys γ -FeNiMn (Refs. 1, 2) and γ -FeNiCr (Ref. 3) Binary alloy systems are naturally of greatest theoretical interest. Ni-Fe and Ni-Mn alloys could be a good example, where the existence of a mixed exchange interaction between the atoms has been shown experimentally.⁴ Unfortunately, however, a full picture of the ferro-antiferromagnetic transition in these systems is not observed as a result of the fcc \rightarrow bcc and fcc \rightarrow fct structural transformations.

In this connection our attention was drawn to the Co-Mn alloy system, where a concentration ferro-antiferromagnetic transition is realized within the confines of the fcc crystal lattice. However, because of the few studies of these alloys and of the contradictory experimental facts,⁵⁻⁷ the nature of this transition remains unexplained. In fact, whereas there were no doubts that cobalt alloys with up to 20 at.% Mn are ferromagnetic,⁵ while above 45% they are antiferromagnetic,⁶ nothing definite is known about the magnetic state of the alloys at all in the composition range 30–40 at.%. Antiferromagnetism was suggested by Matsui *et al.*⁵ and mictomagnetism by Rhiger *et al.*⁷ The features of the γ - ϵ transformation were also not taken into account in the range of ferromagnetic alloys, the boundaries of which were not established in this alloy system.

The present work is a broadly planned study of the magnetic state of cobalt-manganese alloys, carried out in order to construct a full magnetic phase diagram by magnetic and neutron diffraction methods.

METHOD OF INVESTIGATION

For carrying out this study, Co-Mn alloys (20 compositions) were prepared with manganese content from 10 to

52 at.% Pure cobalt and electrolytic manganese were used as the starting components. Fusion was carried out in an electric furnace in an argon atmosphere. Chemical analysis showed that all the alloys had a composition close to that intended.

Ingots of the alloys were cut into two parts and were forged into 8–10 mm diameter rods which then underwent a homogenizing anneal in a helium atmosphere at 1000 °C for ~ 100 h. For measuring the temperature dependence of the magnetization of the alloys, cylindrical specimens of 3 mm diameter and 3 mm long were prepared, and the samples for measuring the dynamical ac susceptibility had a diameter 2 mm and a length 15 mm. Neutron diffraction investigations were carried out both on cylindrical specimens with diameter 8 mm and length 60 mm, and on powders prepared from these alloys by filing.

The initial state of all the specimens corresponded to a long soaking at 1300 K in an argon atmosphere and subsequent cooling in a quartz tube outside the furnace. According to an x-ray phase analysis, all specimens in the initial state at room temperature had a face centered cubic structure.

Measurements of magnetization curves were carried out with a vibration magnetometer in the temperature range 4.2–1200 K in magnetic fields up to $4 \times 10^5 \text{ A}\cdot\text{m}^{-1}$. The Curie temperature of the alloys was determined in a special apparatus from the break in the temperature dependence of the magnetization, measured in small fields ("kink" method). The static magnetic susceptibility was measured by the Faraday method in a field of $2.15 \times 10^5 \text{ A}\cdot\text{m}^{-1}$ and in the temperature range 4.2–300 K. The real and imaginary parts of the dynamic susceptibility and also the nonlinear susceptibility were measured over the same temperature range using a specially constructed apparatus described elsewhere.⁸ Measurements were made at an ac frequency of 36 Hz in the earth's field and in an external steady field up to $1.59 \text{ A}\cdot\text{m}^{-1}$. The accuracy in temperature measurement was not worse than 0.5 K in all cases.

Neutron-diffraction investigations were carried out using a diffractometer installed in one of the horizontal channels of the IVV-2 reactor. A monochromatic neutron beam ($\lambda = 0.181$ nm) was obtained by reflection from the (111) plane of a deformed germanium single crystal. The intensity of second order reflections was then zero, since Co-Mn alloys in the composition range studied came close to "zero scattering matrix" ($b_{\text{Co}} = 0.25 \times 10^{-5}$ nm, $b_{\text{Mn}} = -0.36 \times 10^{-5}$ nm). The scattered neutron intensity measured near the (110) reflection was therefore only of magnetic character, which appreciably increased the sensitivity of our method for revealing weak coherent reflections.

EXPERIMENTAL RESULTS AND DISCUSSION

1. Ferromagnetism and structural transformations in cobalt-manganese alloys

To determine the region of existence of alloys with ferromagnetic long-range order and also to establish the boundaries of a structural transformation in the Co-Mn system, the temperature dependences of magnetization in the maximum magnetic field of 8×10^5 A·m⁻¹ and the magnetization curves at fixed temperatures were studied. The most typical $\sigma(T)$ dependences are shown in Fig. 1, from which shows the existence of hysteresis in the magnetic properties, giving evidence that structural transformations take place in the alloys. When alloys with 10 and 20 at. % Mn are cooled, the magnetization undergoes a sharp fall in the region of 660 and 280 K respectively (this result is only shown for the alloy with 20 at. % Mn in Fig. 1). Consequently, the low-temperature ϵ -phase which has a hexagonal lattice has a smaller magnetization than the high-temperature γ -phase.

A different picture is observed for the alloys with 25, 27 and 29 at. % Mn (curves 2, 3 and 4 in Fig. 1). On lowering the specimen temperature to the region of the $\gamma \rightarrow \epsilon$ structural transformation, the magnetization increases and its high value is preserved on further heating the specimens to the temperatures of the $\epsilon \rightarrow \gamma$ transformation. The conclusion that follows from this is that for the compositions 25–29 at. % Mn the magnetization of the ϵ phase is higher than of the γ phase, while the alloy for which the magnetizations of the γ and ϵ phases are equal corresponds to ~ 23.5 at. % Mn.

The temperature dependences of the magnetization of the Co-Mn alloys studied are rather smeared in the region of

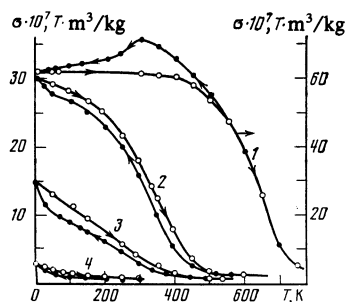


FIG. 1. Temperature dependences of the saturation magnetization ($H = 7.96 \times 10^5$ A·m⁻¹) for Co-Mn alloys with Mn content (at. %): 1) 20; 2) 25; 3) 27; 4) 29, measured on increasing (●) and decreasing (○) the temperature.

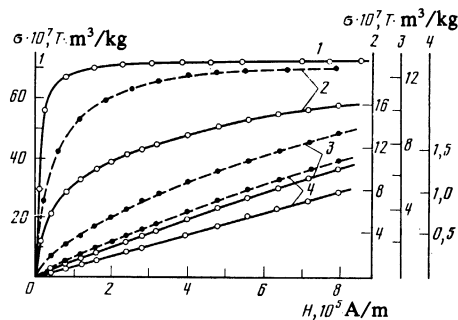


FIG. 2. Magnetization curves for Co-Mn alloys with Mn content (at. %): 1) 20; 2) 25; 3) 27; 4) 29, measured at 300 K (solid lines) and at 200 K (dashed lines).

the Curie temperature, so that the latter cannot be estimated. We used the "kink" method for greater definiteness and established that the extreme composition for which the break in the temperature dependence of magnetization near T_c can be recorded is an alloy with 25 at. % Mn. This can therefore be considered the limiting ferromagnetic alloy in the Co-Mn system.

Measurements of magnetization curves were carried out at several fixed temperatures. Some characteristic magnetization curves at 300 and 200 K are shown in Fig. 2. It can be seen that the alloy with 20 at. % Mn (curve 1) is a good ferromagnet with fairly high remanent magnetization, while the alloys with 27 and 29 at. % Mn have the form characteristic of superparamagnets and paramagnets. The alloy with 25 at. % Mn occupies an intermediate position. Remanent magnetization can still be resolved on the magnetization curves obtained at 200 and 300 K, although the $\sigma(H)$ curves remind one strongly of the Langevin behavior. Having a family of $\sigma(H)$ curves obtained at different temperatures, we could establish the transition temperature from the superparamagnetic to paramagnetic state to a certain accuracy (~ 50 K). According to our estimates it corresponds to that temperature region where the $\sigma(H)$ curves in fields up to 10^6 A·m⁻¹ become straight lines. Such a situation was observed for the alloys with 25, 27, and 29 at. % Mn at roughly 500, 440, and 250 K respectively.

The dimensions of the superparamagnetic clusters were calculated from the Langevin-like magnetization curves, using the well known procedure and this turned out to be within the limits of 8.0–20 nm. The dimensions of the clusters naturally increase on lowering the temperature of the alloy and on the approach of its composition to the ferromagnetism region.

It was thus possible to establish the region of existence of ferromagnetism and superparamagnetism and also the boundaries of the γ - ϵ transformation and the extent of its influence on the magnetization, from studying the magnetic properties of alloys with Mn content from 0 to 30 at. %.

2. Antiferromagnetism and superantiferromagnetism in Co-Mn alloys

The investigations of the phase diagram in the antiferromagnetic range of alloys were mainly carried out by neu-

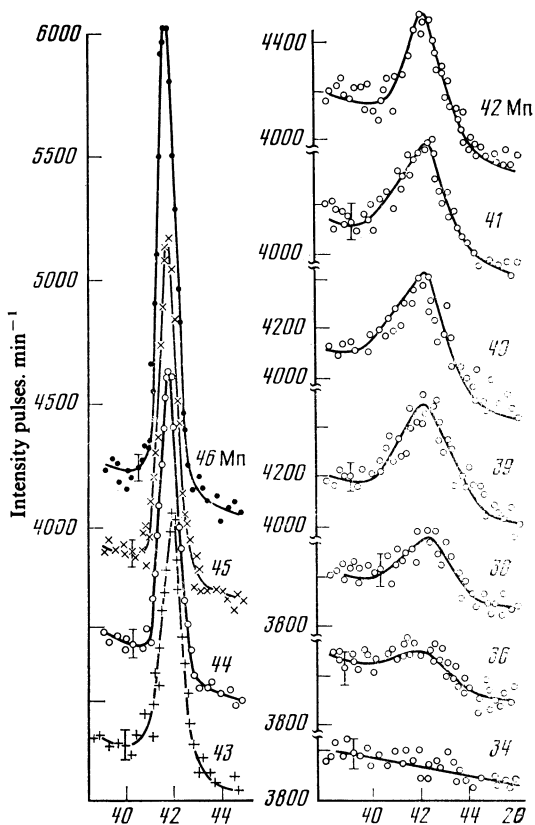


FIG. 3. Antiferromagnetic (110) reflection from Co-Mn alloys with different manganese content (the numbers against the curves are in at. %).

tron diffraction. For this purpose the concentration and temperature dependences of the antiferromagnetic (110) reflection were studied, its intensity being entirely due to the magnetic properties.

The results of measuring the concentration dependence of the intensity of the (110) antiferromagnetic reflection at 4.2 K are shown in Fig. 3. It can be seen that for alloys with manganese content greater than 43 at. %, a fairly narrow coherent (110) reflection is observed, while for alloys with 35–42 at. % Mn this reflection is appreciably broader and is produced by coherent neutron scattering from particles of small dimensions. The concentration dependence of the width of the (110) reflection at its half-height at 4.2 K is

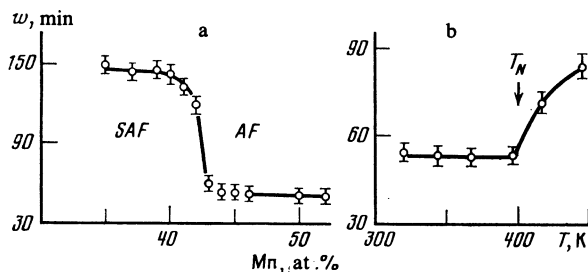


FIG. 4. The dependence of the width of the (110) diffraction reflection at its half height for Co-Mn alloys on concentration (a) and temperature (b) for an alloy of composition $\text{Co}_{55}\text{Mn}_{45}$.

shown in Fig. 4, a, from which the existence of two horizontal sections can be seen, passing from one to the other at a critical concentration ($c_{cr} = 43$ at. % Mn).

It was noted when studying the temperature dependence of the intensity of the antiferromagnetic (110) reflection for alloys with manganese content greater than 43 at. % that on raising the temperature, a reduction in the integrated intensity of the (110) reflection takes place, first without a change in its width, but an abrupt broadening is then observed at a certain temperature T_N (Fig. 4, b). Total vanishing of the intensity is observed at another higher temperature, T_{SAF} . The existence of a broad (110) reflection for alloys of certain compositions and temperatures is evidence of the presence of coherent neutron scattering from antiferromagnetic regions of finite dimensions, the magnitude of which can be evaluated from the formula

$$L = 0,94\lambda / \Delta w \cos \theta, \quad (1)$$

where λ is the wavelength, θ the scattering angle, and Δw the broadening of the line relative to the instrumental line width obtained for alloys in the presence of infinite antiferromagnetically ordered clusters. Calculation according to Eq. (1) gives the magnitude of the antiferromagnetic blocks as ~ 8 – 12 nm.

The temperatures for the disappearance of antiferromagnetic order in antiferromagnetic clusters of both infinite and finite dimensions were established on the basis of the neutron diffraction experiments carried out.

As was shown earlier,⁹ the state of an antiferromagnet broken up into clusters of finite dimensions can be identified with the superantiferromagnetism state predicted by Petrákovskii *et al.*¹⁰ These authors,¹⁰ by considering the magnetic phase diagram of an Ising magnet with stochastically mixed exchange couplings and strongly expressed antiferromagnetic exchange, came to the conclusion that in some concentration and temperature regions the antiferromagnetic long-range order becomes unstable, but does not disappear entirely, as in a paramagnet, but exists in clusters of dimensions ~ 10 nm. Such a mixed state of a paramagnet and antiferromagnetic clusters of finite size was called superantiferromagnetic by the authors. It is realized in alloys above the Néel temperature T_N or the freezing temperature of a spin glass and thereby differs from the definition of "superantiferromagnetism" introduced by Néel for describing the magnetic behavior of finely dispersed antiferromagnetic NiO particles.

3. The magnetic state of alloys in the transition region

a) 25–33 at. % Mn. Studies of the dynamic (ac) and static (dc) susceptibilities were undertaken to elucidate the basic magnetic state of alloys in the region intermediate between ferromagnetic and antiferromagnetic long-range order, i.e., in the concentration range 25–42 at. % Mn. The results of these measurements are shown in Figs. 5 and 6. It can be seen that the ac susceptibility (Fig. 5) of alloys with manganese content 25–30 at. % has a maximum at temperature T_M , while the dc susceptibility (Fig. 6) shows the effect of thermomagnetic prehistory.¹ These features of the behav-

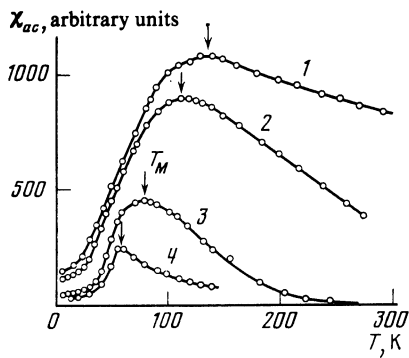


FIG. 5. Temperature dependences of the ac susceptibility of Co-Mn alloys with manganese content (at. %): 1) 25; 2) 27; 3) 29; 4) 30.

ior of the ac and dc susceptibilities usually characterize the transition of the system into the spin-glass state. However, in the present case of Co-Mn alloys, the smooth decrease of the ac susceptibility above T_M (Fig. 5) and the clearly evident shift of its maximum in the low temperature direction with an increase of the external magnetic field (Fig. 7) turned out to be unusual.

There were no such effects in the alloys we studied earlier with a spin glass state.^{2,3} Additional investigations not only of the real but also of the imaginary part of the magnetic susceptibility and, in addition, of the temperature dependence of the nonlinear susceptibility were therefore carried out to elucidate the nature of these features.

The magnetization of a magnetic material following application of a small alternating magnetic field h can in the general case be represented in the form of a series

$$m = m_0 + \chi_0 h + \chi_1 h^2 + \chi_2 h^3 + \dots, \quad (2)$$

where m_0 is the spontaneous magnetization, χ_0 is the linear and χ_1, χ_2, \dots the nonlinear susceptibilities, and h is the alternating magnetic field:

$$h = h_0 \sin \omega t. \quad (3)$$

Since there is no long-range order in the studied Co-Mn

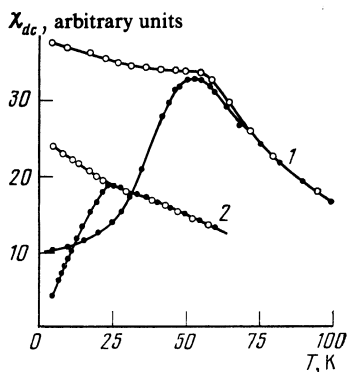


FIG. 6. Temperature dependences of the dc susceptibility of Co-Mn alloys with manganese content (at. %): 1) 30; 2) 32, measured in a field of $7.96 \times 10^2 \text{ A} \cdot \text{m}^{-1}$ in specimens cooled to 4.2 K without a magnetic field (●) and in the measuring field (○).

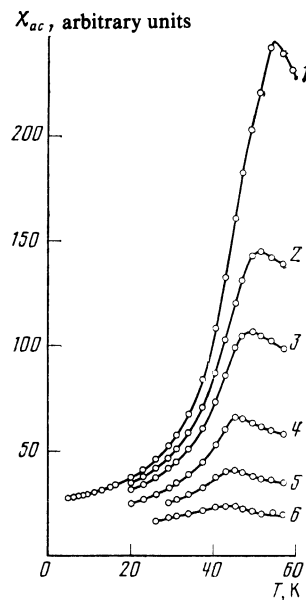


FIG. 7. Temperature dependences of the ac susceptibility of a $\text{Co}_{70}\text{Mn}_{30}$ alloy, measured in fields ($\text{A} \cdot \text{m}^{-1}$): 1) 48; 2) 7.96×10^3 ; 3) 1.59×10^4 ; 4) 3.98×10^4 ; 5) 7.96×10^4 ; 6) 1.59×10^5 .

alloys in the transition region, Eq. (2) simplifies and takes the form

$$m = \chi_0 h + \chi_2 h^3 + \dots \quad (4)$$

Measuring the dynamic magnetic susceptibility at the first and third harmonics, χ_0 and χ_2 can then be determined, where χ_0 in its turn is the complex quantity

$$\chi_0 = \chi_0' - i\chi_0''. \quad (5)$$

As has been shown by Taniguchi *et al.*¹² and Saito *et al.*,¹³ the imaginary part χ_0'' , of the susceptibility, which characterizes the magnetic dynamics of the system, and also the nonlinear susceptibility χ_2 , have a critical behavior near the spin glass-paramagnet transition. They are very sensitive to critical fluctuations and can change by several orders of magnitude in a narrow temperature region. The similarity law (static scaling) then applies. The effective relaxation time for the magnetic system shows a similar behavior, and is defined in the Debye approximation as

$$\tau_0 = \chi_0'' / \omega \chi_0'. \quad (6)$$

A comparison of the results of studying the real and imaginary parts of the magnetic susceptibility and also of the nonlinear susceptibility and of the calculated relaxation time τ_0 for a Co-Mn alloy with 29 at. % Mn is shown in Fig. 8. Completely analogous curves exist for all the other alloys which we investigated. It can be seen that the maxima in χ_0' and χ_0'' coincide in temperature and the shape of the curves is one and the same. The nonlinear susceptibility behaves in a very similar way. The relaxation time does not then diverge at the temperature corresponding to the maximum of the imaginary part of the magnetic susceptibility.

The single conclusion which can thus be drawn from

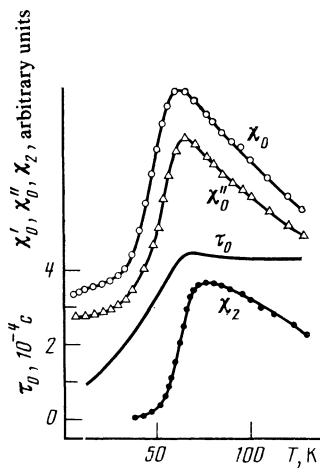


FIG. 8. Temperature dependences of the dynamic susceptibility of a $\text{Co}_{71}\text{Mn}_{29}$ alloy: χ'_0 —the real part, χ''_0 —the imaginary part, χ_2 —the non-linear part; τ_0 —the relaxation time of the magnetic system.

this fact is that in cobalt-manganese alloys a cooperative process of freezing of the spin system does not take place in the transition region, but a typical process of blocking of superparamagnetic clusters takes place which starts at the temperature T_M . Other observed effects can also be explained on the basis of ideas about the blocking of superparamagnetic clusters, namely the relaxation time below T_M and the shift of T_M to lower temperatures with increasing external magnetic field.

In fact, according to Néel¹⁴

$$\tau = \tau_0 \exp [(E_a + \mu_a H) / kT_B], \quad (7)$$

where τ is the observation time, $E_a = K_{\text{eff}} V$ is the effective anisotropy energy of a cluster of volume V with effective anisotropy constant K_{eff} , H is the external steady magnetic field, and μ_a is the effective magnetic moment of the cluster.

Since there is always a cluster distribution in size large-volume clusters are blocked first when the temperature is lowered. The remaining unblocked clusters then naturally have a smaller relaxation time and make their contribution to the response of the system to an external excitation at lower temperatures. A reduction in temperature is accompanied by further blocking of clusters with a reduction in the effective relaxation time of the magnetic system. An external magnetic field at the given temperature then promotes blocking of clusters of smaller volume, which is equivalent to a lowering of the effective relaxation time of the unblocked clusters. The concentration effect of the change of T_M (Fig. 5) is also understandable. The smaller the manganese concentration in the alloy, the closer is the alloy to the ferromagnetic region and the larger is the effective size of the superparamagnetic clusters and the higher the initial temperature for blocking these clusters.

b) 35–42 at. % Mn. We now turn to another, no less important, composition region (33–42 at. % Mn), adjacent to pure antiferromagnetism. As was indicated above, these alloys show a superantiferromagnetic behavior. It seemed interesting to trace the evolution of the magnetic state of

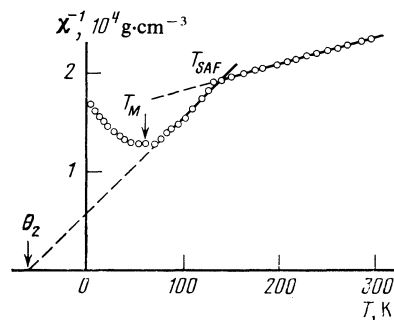


FIG. 9. The temperature dependence of the inverse susceptibility of a $\text{Co}_{66}\text{Mn}_{34}$ alloy.

such alloys on lowering the temperature. The static magnetic susceptibility was studied for these purposes. It turned out that there is a maximum in the $\chi(T)$ temperature plot of alloys containing 34, 36, and 37 at. % Mn which occurs at 60, 70, and 75 K respectively. No singularity was observed in the susceptibility at high temperatures in all the other alloys with larger manganese content, in agreement with the results of Matsui *et al.*⁵ and Rhiger *et al.*⁷ The main feature of these curves is that the temperature of the susceptibility maximum does not coincide with the superantiferromagnetism temperature: the latter is appreciably higher. However, there is an anomaly in the behavior of χ^{-1} at the point T_{SAF} . Typical temperature dependences of the inverse susceptibility are shown, for example, in Fig. 9 for an alloy with 34 at. % Mn. Attention is called to the existence on the $\chi^{-1}(T)$ curve of two linear sections having different slopes relative to the temperature axis, and, correspondingly, different paramagnetic temperatures θ_1 and θ_2 . The temperature 140 K at which the two straight lines intersect coincides roughly with T_{SAF} , while the temperature of the maximum susceptibility (~ 60 K) corresponds to the start of the blocking of antiferromagnetic clusters. We note, however, that the appearance of a maximum in the temperature dependence of the static susceptibility is typical only of alloys with antiferromagnetism in finite-size clusters. The larger the size of the cluster, the less pronounced this maximum. The susceptibility maximum is not observed at all for alloys with manganese content more than 40 at. %.

Such a result is explained, within the framework of Néel's theory,¹⁴ by the fact that the odd number of antiferromagnetic layers in a cluster starts to play a role in antiferromagnetic clusters of small dimensions, leading to the appearance of magnetization of such particles and to their superparamagnetic behavior with corresponding blocking at T_B , where the maximum susceptibility is observed. The increase in the size of the antiferromagnetic clusters cancels this effect and is accompanied by a smearing out of the susceptibility singularities both near their blocking temperature and at the Néel point. This conclusion also agrees well with the theoretical predictions.¹⁰

4. Magnetic phase diagram for Co–Mn alloys

The complete magnetic phase diagram for Co–Mn alloys constructed on the basis of the experimental investiga-

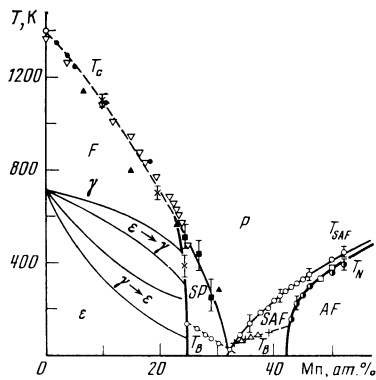


FIG. 10. The magnetic phase diagram of Co-Mn alloys: F—ferromagnetism, AF—antiferromagnetism, P—paramagnetism, SP—superparamagnetism, SAF—superantiferromagnetism. The dashed curves correspond to second order phase transition lines, the solid lines to first order. Also shown are the T_B lines for blocking of the superparamagnetic and superantiferromagnetic states; \blacktriangle Ref. 5, \square Ref. 6, $+$ Ref. 7, \bullet Ref. 15, ∇ Ref. 18, \times , \blacksquare , \circ , \triangle , \odot results of the present work.

tions carried out is shown in Fig. 10. It shows the regions of existence of ferromagnetic (F) and antiferromagnetic (AF) long-range order, also of superparamagnetism (SP) and superantiferromagnetism (SAF) states, which are mixtures of ferro- and antiferromagnetic clusters with the paramagnetic phase, respectively. The experimental points of not on the SP-P and SAF-P lines are not very accurate, but the existence of the lines as such is of no doubt.

As can be seen from Fig. 10, there is no region of overlap of the ferromagnetic and antiferromagnetic states on the magnetic phase diagram. There is so to speak an independent jointing of the phase transition lines both from the ferromagnetism and the antiferromagnetism directions. In both cases tricritical behavior is found, the result of which is the transformation of the second-order phase-transition line into two first-order phase-transition lines, between which a mixture of two phases is contained, designated here as a superparamagnet and a superantiferromagnet. On lowering the temperature these states are "frozen-in" by blocking of the ferro- and antiferromagnetic clusters on the corresponding T_B lines indicated in the diagram.

The reason for such a form of magnetic phase diagram for Co-Mn alloys must be sought in the nature of the exchange interaction between the atoms. For this we turn to an analysis of the concentration dependence of the mean magnetic moment, shown in Fig. 11 according to earlier results in the literature¹⁵⁻¹⁸ and the present investigation. As can be seen, the mean magnetic moment in the γ and ϵ phases decreases on adding manganese to cobalt, i.e., $d\bar{\mu}/dc_{Mn} < 0$ in the initial section. It can be assumed from this that $J_{CoMn} < 0$ on top of the well known relations $J_{CoCo} > 0$ and $J_{MnMn} < 0$. In this sense Co-Mn alloys differ from Ni-Fe and Ni-Mn alloys, where $J_{NiFe} > 0$ and $J_{NiMn} > 0$ and the initial derivative $d\bar{\mu}/dc$ is positive.⁴ Consequently, $\bar{\mu}$ decreases in Co-Mn alloys because of the antiferromagnetic position of manganese atoms relative to cobalt atoms. The value of the local magnetic moment at the manganese atoms for the γ and ϵ phases then amounts to about (2.5–2.9) μ_B in the concen-

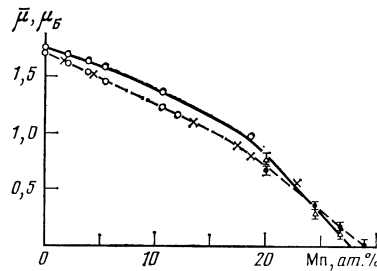


FIG. 11. The concentration dependence of the mean magnetic moment of Co-Mn alloys for the γ (solid line) and ϵ (dashed line) phases: \circ Ref. 17, \times Ref. 16; \triangle , \bullet results of the present work.

tration range from 0 to 20 at. % Mn. But above 20 at. % Mn, $\bar{\mu}$ decreases also because of the reduction in the magnetic moment of the cobalt atoms, the magnitude of which is sensitive to the immediate surroundings of the manganese atoms.

All this together leads to the fact that the fraction of antiferromagnetically interacting Co-Mn and Mn-Mn pairs increases continuously with increase in the Mn content, while the fraction of ferromagnetically interacting Co-Co pairs falls at first gradually and then sharply, and becomes zero near the concentration ~ 27 at. % Mn. Based on this, the Co-Mn alloy system can be considered as a typical Ising magnet in which, for certain concentrations, antiferromagnetic interaction appreciably predominates over the ferromagnetic. This evidently creates the conditions for the formation of the superantiferromagnetic state which, according to Petrakovskii *et al.*,¹⁰ is realized at a ratio of the antiferromagnetic interaction constant to the ferromagnetic constant equal to 20.

CONCLUSIONS

As a result of the combination of magnetic and neutron diffraction studies carried out in this work, a magnetic phase diagram for Co-Mn alloys in the region of the ferro-antiferromagnetic transition could be constructed. The main feature of this diagram is that the ferromagnetic and antiferromagnetic states do not overlap and an intermediate spin-glass state does not exist. An independent jointing of two homogeneous phase diagrams is observed, on the ferromagnetic and antiferromagnetic sides on which there is a clearly evident tricritical behavior. The existence of a region of superparamagnetism and superantiferromagnetism is evidence of this.

There can be no doubt that on lowering the temperature, all the singularities of the ac and dc susceptibilities are due not to a phase transition into a spin glass state, but to a gradual blocking of ferromagnetic and antiferromagnetic clusters in the random anisotropy field. The magnetic properties of such "frozen-in" regions of long range-magnetic order with finite dimensions is in many ways analogous to the properties of spin glass. But unlike the latter, there are no critical phenomena pointing to the cooperative nature of the phase transition at temperatures corresponding to the maximum of the dynamic and static susceptibility. Such states should be well described quantitatively within the framework of Néel's theory.¹⁴ However, our attempts at such an

analysis for the present system ended unsuccessfully. For example, the field dependence of the blocking temperature is not described by the law $T(H)/T(0) = (1 - H/H_k)^2$, as should follow from theory.¹⁹ The quantitative description of such frozen-in superparamagnets and superantiferromagnets thus requires a detailed theoretical analysis.

The authors express their deep gratitude to L. V. Smirnov for preparation of the alloys.

¹A. Z. Men'shikov, V. A. Kazantsev, and N. N. Kuz'min, *Zh. Eksp. Teor. Fiz.* **71**, 648 (1976) [*Sov. Phys. JETP* **44**, 341 (1976)].

²A. Z. Menshikov, P. Burllet, A. Chamberod, and J. L. Tholence, *Solid State Commun.* **39**, 1093 (1981).

³A. Z. Men'shikov, G. A. Takzei, and A. E. Teplykh, *Fiz. Met. Metalloved.* **54**, 465 (1982) [*Phys. Met. and Metallogr. (GB)* **54**, No. 3, 41 (1982)].

⁴A. Z. Menshikov, V. A. Kazantsev, N. N. Kuzmin, and S. K. Sidorov, *J. Magnet. and Mag. Mat.* **1**, 91 (1975).

⁵M. Matsui, T. Ido, K. Sato, and K. Adachi, *J. Phys. Soc. Jpn.* **28**, 791 (1970).

⁶K. Adachi, K. Sato, M. Matsui, and S. Mitani, *J. Phys. Soc. Jpn.* **35**, 426 (1973).

⁷D. R. Rhiger, D. Müller, and P. A. Beck, *J. Magnet. and Mag. Mat.* **15-18**, 165 (1980).

⁸A. M. Kostyshin and G. A. Takzei, Preprint IFM, 4.85 (1985).

⁹A. Z. Men'shikov and Yu. A. Dorofeev, *Pis'ma Zh. Eksp. Teor. Fiz.* **40**, 59 (1984) [*JETP Lett.* **40**, 791 (1984)].

¹⁰G. A. Petrakovskii, E. V. Kuz'min and S. S. Aplesnin, *Fiz. Tverd. Tela (Leningrad)* **24**, 3298 (1982) [*Sov. Phys. Solid State* **24**, 1872 (1982)].

¹¹S. V. Vonsovskii, *Magnetism*; 2 vols., Halsted, New York (1975).

¹²T. Taniguchi, H. Matsuyama, S. Chikazawa, and Y. Miyako, *J. Phys. Soc. Jpn.* **52**, 4323 (1983).

¹³T. Saito, C. J. Sandberg, and Y. Miyako, *J. Phys. Soc. Jpn.* **52**, 3170 (1983).

¹⁴L. Néel, *Adv. Phys.* **4**, 191 (1955).

¹⁵J. Crangle, *Philos. Mag.* **2**, 659 (1957).

¹⁶C. Sadron, *Ann. Phys. (Paris)* **17**, 371 (1932).

¹⁷J. S. Kouvel, *J. Phys. Chem. Solids* **16**, 107 (1960).

¹⁸H. Masumoto, S. Sawaya, and M. Kikuchi, *Nippon Kinzaky Gakkai-Si*, **33**, 999 (1969).

¹⁹E. P. Wohlfarth, *J. Phys.* **F10**, L241 (1980).

Translated by R. Berman